AFRL-RX-WP-JA-2017-0197

DIELECTRIC PERFORMANCE OF HIGH PERMITIVITY NANOCOMPOSITES: IMPACT OF POLYSTYRENE GRAFTING ON BaTiO$_3$ AND TiO$_2$ (POSTPRINT)

Christopher A. Grabowski
UES

Scott P. Fillery, Hilmar Koerner, Maxim Tchoul, Lawrence Drummy, Michael F. Durstock, and Richard A. Vaia
AFRL/RX

Christopher W. Beier and Richard L. Brutchey
University of Southern California

27 July 2016
Interim Report

(STINFO COPY)

AIR FORCE RESEARCH LABORATORY
MATERIALS AND MANUFACTURING DIRECTORATE
WRIGHT-PATTERSON AIR FORCE BASE, OH 45433-7750
AIR FORCE MATERIEL COMMAND
UNITED STATES AIR FORCE

REPORT DOCUMENTATION PAGE

Form Approved
OMB No. 0704-0188

The public reporting burden for this collection of information is estimated to average 1 hour per response, including the time for reviewing instructions, searching existing data sources, gathering and maintaining the data needed, and completing and reviewing the collection of information. Send comments regarding this burden estimate or any other aspect of this collection of information, including suggestions for reducing this burden, to Department of Defense, Washington Headquarters Services, Directorate for Information Operations and Reports (0704-0188), 1215 Jefferson Davis Highway, Suite 1204, Arlington, VA 22202-4302. Respondents should be aware that notwithstanding any other provision of law, no person shall be subject to any penalty for failing to comply with a collection of information if it does not display a currently valid OMB control number. **PLEASE DO NOT RETURN YOUR FORM TO THE ABOVE ADDRESS.**

1. REPORT DATE *(DD-MM-YY)*	2. REPORT TYPE	3. DATES COVERED *(From - To)*
27 July 2016	Interim	4 August 2010 – 15 June 2015

4. TITLE AND SUBTITLE

DIELECTRIC PERFORMANCE OF HIGH PERMITIVITY NANOCOMPOSITES: IMPACT OF POLYSTYRENE GRAFTING ON BaTiO$_3$ AND TiO$_2$ (POSTPRINT)

5a. CONTRACT NUMBER
FA8650-09-D-5037-0017

5b. GRANT NUMBER

5c. PROGRAM ELEMENT NUMBER
62102F

6. AUTHOR(S)

1) Christopher A. Grabowski – UES

2) Scott P. Fillery, Hilmar Koerner, Maxim Tchoul, Lawrence Drummy, Michael F. Durstock, and Richard A. Vaia -AFRL/RX

(continued on page 2)

5d. PROJECT NUMBER
4348

5e. TASK NUMBER

5f. WORK UNIT NUMBER
X0LW

7. PERFORMING ORGANIZATION NAME(S) AND ADDRESS(ES)

1) UES, Inc.
4401 Dayton Xenia Rd
Beavercreek, OH 45432

2) AFRL/RX
Wright-Patterson AFB, OH 45433

(continued on page 2)

8. PERFORMING ORGANIZATION REPORT NUMBER

9. SPONSORING/MONITORING AGENCY NAME(S) AND ADDRESS(ES)

Air Force Research Laboratory
Materials and Manufacturing Directorate
Wright-Patterson Air Force Base, OH 45433-7750
Air Force Materiel Command
United States Air Force

10. SPONSORING/MONITORING AGENCY ACRONYM(S)
AFRL/RXAS

11. SPONSORING/MONITORING AGENCY REPORT NUMBER(S)
AFRL-RX-WP-JA-2017-0197

12. DISTRIBUTION/AVAILABILITY STATEMENT
Distribution Statement A. Approved for public release: distribution unlimited.

13. SUPPLEMENTARY NOTES
PA Case Number: 88ABW-2016-3731; Clearance Date: 27 Jul 2016. This document contains color. Journal article published in Nanocomposites, Vol. 2, No. 3, 22 Sep 2016. © 2016 US Government. The U.S. Government is joint author of the work and has the right to use, modify, reproduce, release, perform, display, or disclose the work.
The final publication is available at http://dx.doi.org/10.1080/20550324.2016.1223913

14. ABSTRACT *(Maximum 200 words)*
Polymer nanocomposites are a promising concept to improve energy storage density of capacitors, but realizing their hypothetical gains has proved challenging. The introduction of high permittivity fillers often leads to reduction in breakdown strength due to field exclusion, which intensifies the applied electric field within the polymer matrix near nanoparticle interfaces. This has prompted research in developing new nanoparticle functionalization chemistries and processing concepts to maximize particle separation. Herein, we compare the dielectric performance of blended nanocomposites to matrix free assemblies of hairy (polymer grafted) nanoparticles (HNPs) that exhibit comparable overall morphology. The dielectric breakdown strength of polystyrene grafted BaTiO3 (PS@BaTiO3) systems was over 40% greater than a blended nanocomposite with similar loading (~25% v/v BaTiO3). Hairy nanoparticles with TiO2 cores followed similar trends in breakdown strength as a function of inorganic loading up to 40% v/v. Dielectric loss for PS@BaTiO3 HNPs was 2–5 times lower than analogous blended films for a wide frequency spectrum (1 Hz to 100 kHz).

15. SUBJECT TERMS
Polymer nanocomposites, Hairy nanoparticles, Dielectric breakdown, Barium titanate, Titanium dioxide

16. SECURITY CLASSIFICATION OF:

a. REPORT	b. ABSTRACT	c. THIS PAGE
Unclassified	Unclassified	Unclassified

17. LIMITATION OF ABSTRACT:
SAR

18. NUMBER OF PAGES
11

19a. NAME OF RESPONSIBLE PERSON (Monitor)
Lawrence Drummy

19b. TELEPHONE NUMBER *(Include Area Code)*
(937) 255-9160

Standard Form 298 (Rev. 8-98)
Prescribed by ANSI Std. Z39-18

REPORT DOCUMENTATION PAGE Cont'd

6. AUTHOR(S)

   3) Christopher W. Beier and Richard L. Brutchey - University of Southern California

7. PERFORMING ORGANIZATION NAME(S) AND ADDRESS(ES)

   3) University of Southern California
      3551 Trousdale Pkwy, Los Angeles, CA 90089

Dielectric performance of high permitivity nanocomposites: impact of polystyrene grafting on BaTiO$_3$ and TiO$_2$

Christopher A. Grabowski[1,2], Scott P. Fillery[1], Hilmar Koerner[1], Maxim Tchoul[1], Lawrence Drummy[1], Christopher W. Beier[3], Richard L. Brutchey[3], Michael F. Durstock[1] and Richard A. Vaia[1]*

[1]Air Force Research Laboratory, Materials and Manufacturing Directorate, Wright-Patterson Air Force Base, OH, USA
[2]UES, Inc, Dayton, OH, USA
[3]Department of Chemistry, University of Southern California, Los Angeles, CA, USA

Abstract Polymer nanocomposites are a promising concept to improve energy storage density of capacitors, but realizing their hypothetical gains has proved challenging. The introduction of high permittivity fillers often leads to reduction in breakdown strength due to field exclusion, which intensifies the applied electric field within the polymer matrix near nanoparticle interfaces. This has prompted research in developing new nanoparticle functionalization chemistries and processing concepts to maximize particle separation. Herein, we compare the dielectric performance of blended nanocomposites to matrix free assemblies of hairy (polymer grafted) nanoparticles (HNPs) that exhibit comparable overall morphology. The dielectric breakdown strength of polystyrene grafted BaTiO$_3$ (PS@BaTiO$_3$) systems was over 40% greater than a blended nanocomposite with similar loading (~25% v/v BaTiO$_3$). Hairy nanoparticles with TiO$_2$ cores followed similar trends in breakdown strength as a function of inorganic loading up to 40% v/v. Dielectric loss for PS@BaTiO$_3$ HNPs was 2–5 times lower than analogous blended films for a wide frequency spectrum (1 Hz to 100 kHz). For content above 7% v/v, grafting the polymer chains to the BaTiO$_3$ significantly improved energy storage efficiency. Overall this study indicates that polymer grafting improves capacitor performance relative to direct blending in likely two ways: (1) by mitigating interfacial transport to lower dielectric loss, irrespective of the dielectric contrast between matrix and nanoparticle, and (2) by restricting particle–particle hot-spots by establishing a finite minimum particle separation when the dielectric contrast between matrix and nanoparticle is large.

Keywords Polymer nanocomposites, Hairy nanoparticles, Dielectric breakdown, Barium titanate, Titanium dioxide
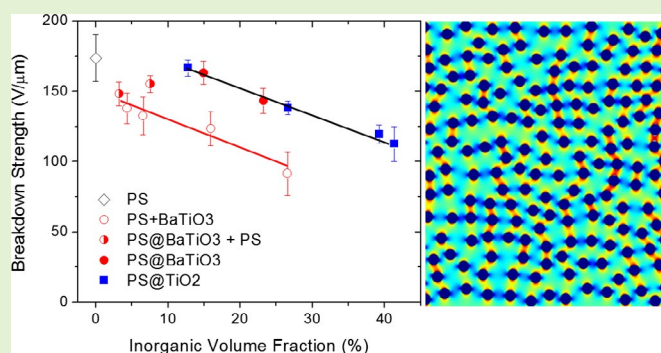
Introduction

Developing polymer nanocomposites (PNCs) for electrostatic capacitors, batteries, and fuel cells has rapidly expanded in recent years. Previous efforts to utilize PNCs for improved capacitive energy storage density (~$\varepsilon_r E_{BD}^2$) have focused on increasing effective composite permittivity (ε_r) by using high permittivity inorganic nanofillers, while simultaneously retaining the high dielectric breakdown strength (E_{BD}) and gradual failure mode of the matrix polymer.[1–3] As evidenced by effective medium theories, permittivity does not scale linearly with inorganic content and significant gains require loadings of dispersed fillers above 20% v/v. At these intermediate to high loading levels, achieving good nanoparticle dispersion – especially in non-polar polymer matrices – is challenging due particle agglomeration during film preparation.[4] Field intensification in the matrix phase, along with extended filler clusters, reduce E_{BD} and enhance charge migration along the interfaces of the percolated fillers. This leads to a decrease in E_{BD} as filler is added to increase ε_r. This behavior, for example, has been observed in finite difference simulations and

---

*Corresponding author, email richard.vaia@us.af.mil

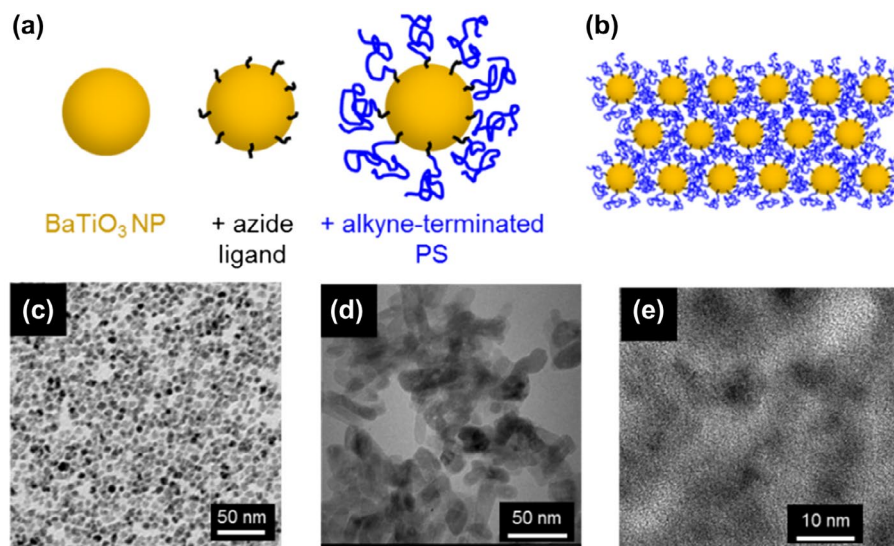Distribution A. Approved for public release (PA): distribution unlimited.

Figure 1 *a* Overview of HNP "click" chemistry synthesis; nanoparticles are functionalized with azide ligands that facilitate grafting of alkyne-terminated polystyrene chains. *b* Illustration of ideal assembled hairy nanoparticle film. TEM images of *c* bare BaTiO$_3$ and *d* TiO$_2$ nanoparticles. *e* Representative TEM of 22% v/v HNP PS@BaTiO$_3$, demonstrating evidence of fractal-like structure

supported experimentally with BaTiO$_3$/ferroelectric polymer blended nanocomposites, where a 50% reduction in breakdown strength was measured for a 40% v/v BaTiO$_3$ PNC film.[5,6]

Numerous motifs have emerged to mitigate particle aggregation (and thus moderate field exclusion), such as aligning anisotropic fillers[7–9] and adopting particles with graded interfaces[10] or core-shell architectures.[11–14] Recent advances in surface initiated ATRP and Cu-catalyzed "click" chemistry have led to an increasingly diverse group of polymer grafted, hairy nanoparticles (HNPs) that feature high ε_r and refractive index core plus a polymer corona with tunable structure.[15–17] Solution cast films of these HNPs without an accompanying polymer matrix have recently been characterized for dielectric performance. Tchoul *et al.* reported that hairy PS@TiO$_2$ matrix free assemblies at 27% v/v inorganic loading have a relative dielectric constant of 6.4, compared to 2.4 for neat PS, while maintaining low dielectric loss similar to PS (tan δ = 0.04 at 1 kHz).[18] X-ray scattering demonstrated excellent particle dispersion with no visible clustering; thus, the deleterious effects of percolation that create conduction pathways and increase dielectric loss were avoided.[19] Similarly, Paniagua *et al.* demonstrated that films of PMMA@BaTiO$_3$ HNPs achieved a maximum extractable energy density of 2 J/cc at intermediate loadings (22% v/v) – a twofold increase over a physically blended nanocomposite at comparable BaTiO$_3$ loading.[20] These findings were attributed to an increased permittivity and greater energy storage efficiency; however, detailed measurements of dielectric breakdown strength and complex permittivity to elucidate the relative impact of the HNP architecture and PNC morphology were not reported.

To gain better insight into the relative roles of morphology and interface architecture, we compare the dielectric strength, complex dielectric permittivity, and energy storage efficiency for traditional blends and matrix free assemblies of polymer-grafted nanoparticles. The nanocomposites all feature polystyrene, a representative low breakdown strength polymer with low permittivity and dielectric loss. Two different

high permittivity nanoparticle cores, TiO$_2$ and BaTiO$_3$, are investigated to establish the broader implications of these findings. Blended nanocomposites and matrix free assemblies of HNPs exhibited similar overall well-dispersed morphologies. While HNP systems are afforded more separation between nanoparticle surfaces due to the high molecular weight surface functionalization, no appreciable improvement in particle ordering was observed.

Dielectric breakdown experimental results, however, show strong dependence on nanoparticle (NP) architecture; grafted high-ε NPs have 40–50% higher breakdown strength (E_{BD}) as compared to analogous traditional blends across 25–40% v/v inorganic loadings. This compliments similar studies of low permittivity contrast systems (e.g. silica NPs and polystyrene; silica NPs and poly methyl methacrylate[21,22]), where the breakdown strength trends of HNPs and blends were comparable with inorganic loading and depended on the relative breakdown strength of the nanoparticle and matrix. In concert with E_{BD}, an appreciable reduction in dielectric loss (up to 1 order of magnitude) was observed for all HNP assemblies, regardless of relative permittivity matching. The combination of E_{BD} enhancement and reduced dielectric loss in high-ε composites translated to increased energy storage efficiencies at intermediate and high loadings (>15% v/v). The overall improvements in dielectric performance for single component HNPs demonstrate the importance of interface architecture when designing nanocomposites for dielectric applications.

Experimental

Materials and synthesis

All nanocomposites were prepared with polystyrene, a non-polar polymer that exhibits relatively low breakdown strength (measured at 175 V/μm in this study) and relative permittivity (2.4 at 1 kHz), but maintains a low dielectric loss (ε' = 10^{-3}) across 1 Hz to 100 kHz frequency. Spherical barium
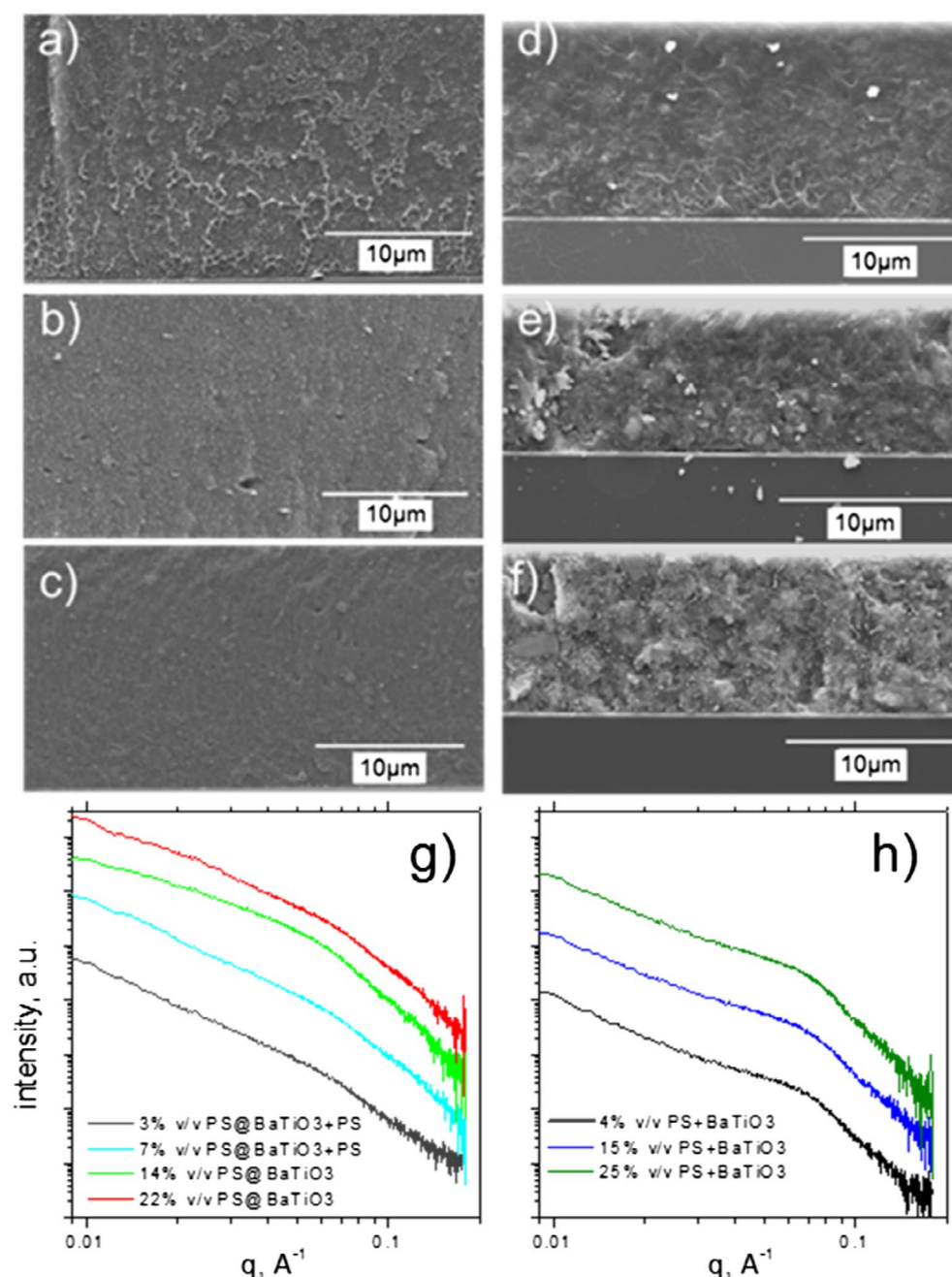
2

Figure 2 *a–c* SEM cross-sections of PS@BaTiO$_3$ HNP films with 3, 14, and 22% v/v inorganic content, respectively. The 3% v/v film contains free polystyrene, while the 14 and 22% samples have no free polymer. *d–f* SEM cross-sections of PS+BaTiO$_3$ blends with 4, 15, and 25% v/v inorganic content, respectively. *g* Small angle X-ray scattering intensity for 3, 7, 14, and 22% v/v PS@BaTiO$_3$ HNP films and *h* 4, 15, 25% v/v PS+BaTiO$_3$ blends

titanate (BaTiO$_3$) nanoparticles, approximately 7.0 ± 1.5 nm in diameter,[23,24] were grafted with polystyrene (102 kg/mol M_w) following a previously reported procedure involving phosphonate coupling and click chemistry[18] (Fig. 1*a–c*, see Supporting Information for full details). In brief, the BaTiO$_3$ NP surface is functionalized with azide ligands in the presence of a CuBr catalyst. These azide end groups react with alkyne-terminated PS chains, completing the "click" reaction. Polystyrene graft densities of 0.036 and 0.022 chains/nm^2 yielded neat HNP samples containing 14 and 22% v/v BaTiO$_3$, respectively. Titanium dioxide (TiO$_2$) nanoparticles were obtained from Ishihara Sangyo Kaisha LTD, Osaka, Japan and are rodlike in

shape, 18 nm in diameter and 40–50 nm in length according to TEM images (Fig. 1*d*). The particles were also grafted with polystyrene (100 kg/mol M_w) using a similar click chemistry approach, fully detailed in Ref.[18]. Graft density was varied from 0.09 to 0.62 chains/nm^2 to generate volume fractions from 12.8% up to 39.1% v/v.

Polymer nanocomposite formation procedures

Matrix-free BaTiO$_3$ HNP films were prepared using the 14 and 22% v/v samples described above. Lower volume fractions of BaTiO$_3$ were obtained by blending the 22% v/v BaTiO$_3$
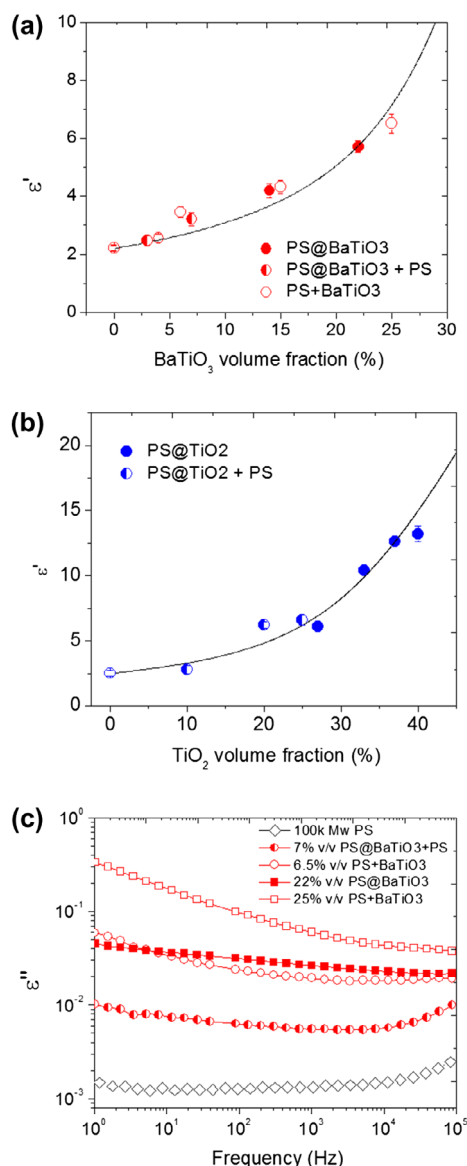
(a)

(b)

(c)

Figure 3 *a* Real dielectric permittivity ε' measured at 1 kHz for PS@BaTiO$_3$ HNPs (filled), HNP blends (half-filled), and PS+BaTiO$_3$ blends (open) and *b* TiO$_2$/PS PNC films. Error bars represent uncertainty in film thickness and impedance measurement reproducibility. Solid lines correspond to the Bruggeman effective medium approximation, assuming ε' = 150 for BaTiO$_3$, 85 for TiO$_2$, and 2.4 for PS. *c* Dielectric loss ε'' measured as a function of frequency for neat polystyrene and select BaTiO$_3$ PNCs. Electrode losses cause the slight increase in ε'' at high frequency

HNPs with free polystyrene of identical molecular weight. Traditional blended nanocomposites, up to 25% v/v azide ligand functionalized BaTiO$_3$ NPs and polystyrene (102 kg/mol M_w), were prepared using high-shear mixing (Ultra-Turrax T18, IKA). All BaTiO$_3$ nanocomposites were solution cast from DMF onto aluminum-coated glass substrates and thermally compressed at 130 °C under 50 MPa pressure for 2 min, yielding films 20–30 μm thick. 10 μm thick films of PS@TiO$_2$ HNPs were flow-coated from chlorobenzene onto aluminum-coated glass substrates.

Dielectric characterization

Dielectric characterization was performed on films with a deposited circular aluminum electrode 6.3 mm^2 in area and 200 nm thick. Dielectric breakdown trials were performed using a 10 kV Spellman SL300 high voltage supply controlled by a ramping circuit. The ramp was set such that a breakdown event occurs at 10–20 s, in accordance to ASTM standard protocol for short-term dielectric strength tests (which corresponded to 10–25 V/s, depending on the sample).[25] Once >1 mA current passes through the device, a silicon rectifier switch activates and breaks the circuit. The breakdown voltages were read from a Fluke 289 multimeter set in peak capture mode. A minimum of 15 tests were conducted for each sample. Note that the areas under breakdown investigation are larger than localized probe measurements previously conducted by the authors (~1 mm^2). Recorded dielectric strengths when sampling an area 1 order larger in magnitude are characteristically 15−30% lower due to a higher probability of probing larger sample flaws.[26] Permittivity, dielectric loss, and energy storage efficiency measurements were all conducted in an N$_2$ purged environment at room temperature employing the same type of electrical contacts used for breakdown experiments. Permittivity was measured at discrete frequencies, swept over the range 1 Hz – 100 kHz at an AC driving voltage of 1 V, using a broadband impedance analyzer (Novocontrol). Energy storage efficiency measurements were conducted on films using a Premier II ferroelectric tester (Radiant Technologies, Inc.), equipped with a Trek 10/10B-HS high voltage amplifier. The applied voltage was a bipolar sinusoidal wave driven at 100 Hz frequency.

Morphology characterization

Electron micrographs of all materials were taken on a Philips CM200 transmission electron microscope from FEI Company operating at 200 kV and on a LVEM5 transmission electron microscope from Delong Instruments operating at a nominal accelerating voltage of 5 kV. Films were microtomed to 75 nm thickness at room temperature using a RMC PowerTome. Individual particles were deposited from solutions on ~15 nm thick amorphous carbon. Small angle X-ray experiments were carried out on a Rigaku S-MAX 3000 3 pinhole SAXS system in transmission mode at a sample to detector distance of 150 cm. CuKα radiation was generated on a Rigaku Ultrax RAG system and focused via a confocal multilayer optic system. Data was corrected for dark current, background, and transmission.

Simulations

Modeling of electric field distribution within the composite was performed using the commercial software packages COMSOL Multiphysics and Mathematica. Nanoparticles were represented as 2D circles of fixed diameter and permittivity, distributed in a uniform dielectric slab. Parallel conductive plates used to apply the external DC field are placed suitably far away to prevent fringing effects and field concentration near sharp corners. A Mathematica routine employing a random number generator distributes particles with a minimum distance between neighboring particles as set by the user. Four cases were investigated: (1) particle separation distance
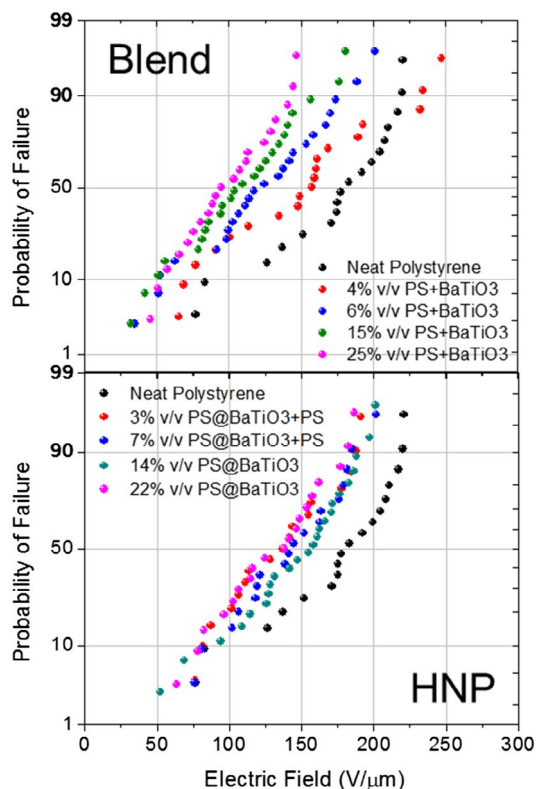
4
Distribution A. Approved for public release (PA): distribution unlimited.

Figure 4 Probability of failure for (top) PS+BaTiO$_3$ blend films and (bottom) PS@BaTiO$_3$ HNP films with increasing inorganic loading. Twenty trials were conducted for each sample using 6.3 mm^2 top electrode contacts
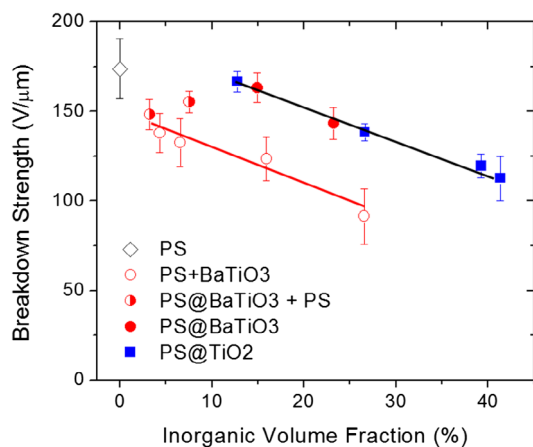

Figure 5 Summary of characteristic breakdown strength E_{BD} as a function of inorganic volume fraction for BaTiO$_3$ and TiO$_2$ PNCs. Error bars represent 1 standard deviation of the collected data. Straight lines are guides showing the trends for blends (red) and matrix-free HNPs (black)

$d \geq 0.25R$, where R is particle radius, (2) $d \geq R$, (3) clustered aggregates, where particles can approach each other as close as possible, and (4) an idealized hexagonal close packing. Case 1 represents a morphology generated by blending low M_w surface functionalized nanoparticles with polymer, while case 2 represents particles grafted with a high M_w polymer brush that ensures a minimum particle separation is maintained. Cases 3 and 4 provide the extremes of disorder and well ordered.

The electric field distributions were plotted as 2D heat maps, where color denotes the magnitude of the local field relative to the applied field. Probabilities of finding regions where field exclusion exceeds E/E_0 were calculated for distributions of 200 particles, which occupy 25% of the area under investigation.

Results and discussion

Drop cast polystyrene-grafted PS@BaTiO$_3$ nanoparticles formed dense, uniform films, as evidenced by SEM cross sections generated from freeze fracturing (Fig. 2a–c). PS + BaTiO$_3$ blended films with comparable inorganic content are shown for comparison (Fig. 2d–f). Overall, the nanoparticle morphology in both systems is comparable, consisting of a random, disordered packing of nanoparticles. The differences in sample morphology were resolved via small angle X-ray scattering; profiles for both types of BaTiO$_3$ PNCs are displayed in Fig. 2g, h. The slight intensity increase at low q implies a distribution of fractal-like aggregates consisting of a few particles. Evidence for few-particle clustering seen throughout PS@ BaTiO$_3$ HNP films is supported by TEM (Fig. 1e). The absence of a pronounced interference peak and intensity decrease in the pattern at intermediate q (0.05 and 0.1 Å) confirms the lack of an ordered lattice of evenly spaced and monodisperse HNPs. One distinction between the systems, however, is a more pronounced Guinier knee (0.07 Å^{-1}) for blends as compared to HNP films. Detailed analysis with a Percus and Yevick hard sphere model[27] confirms BaTiO$_3$ NP size ($r = 3.5$ nm) and the presence of a small fraction of closed packed particles in both systems (see Supporting Information, page 3). The difference in scattering profiles can be explained by a larger particle–particle distance in HNP films due to the covalently attached polystyrene chains. Due to the composite sample dimensions (>10 µm thick) as compared to the nanoparticle size, the HNP architecture does not lead to a highly ordered morphology across the macroscale dimension; instead, it aids in controlling particle spacing and impacts local ordering.

Fig. 3a summarizes the relative dielectric permittivity (ε') at 1 kHz for BaTiO$_3$ and TiO$_2$ polystyrene PNCs (full frequency sweeps are presented in Figs. S3 and S4, Supporting Information). Permittivity rises monotonically for both HNPs and blends with increasing inorganic content. The effective permittivity of the 22% v/v PS@BaTiO$_3$ HNP film was 5.8, compared to 2.4 for neat polystyrene, while PS@TiO$_2$ HNP films with 39% v/v inorganic content showed $\varepsilon' = 12.8$. Therefore, the highest TiO$_2$ loaded sample would improve capacitance by a factor of 5 above a comparable device using neat polystyrene. The permittivity increases observed with BaTiO$_3$ and TiO$_2$ loading are in agreement with Bruggeman effective medium theory,[28] assuming a BaTiO$_3$ relative permittivity of 150 and TiO$_2$ relative permittivity of 80. Dielectric loss (ε') measurements are displayed in Fig. 3b, comparing neat polystyrene to intermediate and high loaded BaTiO$_3$ PNC films, as a function of frequency (see Fig. S4 for PS@TiO$_2$ HNPs). Blends yielded loss values 2–3 times higher at 1 kHz frequency and 6–8 times higher at 1 Hz frequency as compared to HNP samples of similar inorganic content. Comparable behavior was observed previously in silica/polystyrene PNCs near 15% v/v silica loading,[22] where HNP films had dielectric loss nearly 1 order of magnitude smaller than blends at 1 Hz frequency.
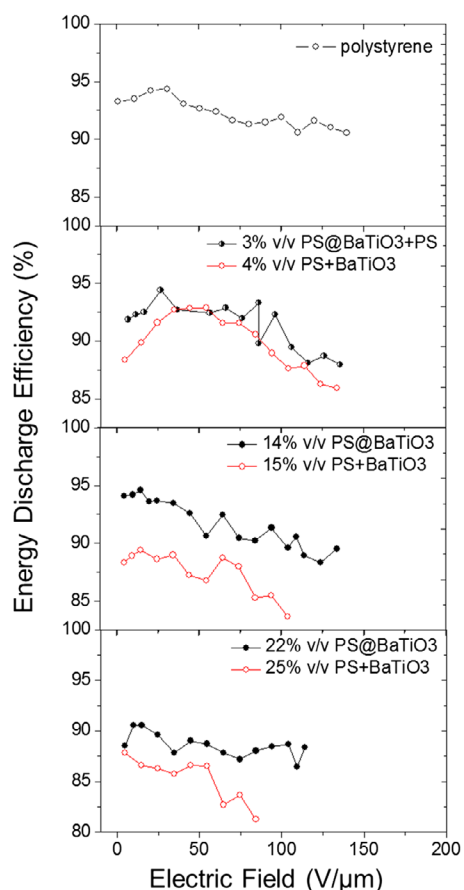
Figure 6 Energy discharge efficiency, calculated from polarization loop experiments, plotted as a function of applied electric field for neat polystyrene and BaTiO$_3$/PS PNCs

In addition to surface passivation, a potential explanation for these results is the reduction of particle clustering achieved in HNPs (as compared to blends). The increased separation of nanoparticle surfaces likely inhibits charge migration and/or hopping between particles.[29] These measurements conclude that adopting an HNP architecture helps reduce loss, especially for films with high inorganic content at low frequencies where blend nanocomposites exhibit the highest loss behavior.

Fig. 4 compares the dielectric failure probability for the BaTiO$_3$ blend and HNP films (PS@TiO$_2$ data is shown in Supporting Information, Fig. S5). The experimental failure data was modeled using a two-parameter Weibull cumulative probability function: $P(E) = 1 - \exp[-(E/E_{BD})^\beta]$ where $P(E)$ is the cumulative probability for failure, E is experimental breakdown strength, E_{BD} reflects the electric field where there is 63.2% probability for failure, and β is the shape parameter associated with the least squares fit of the distribution. The characteristic breakdown strengths obtained for all PNC films are summarized in Fig. 5, plotted as a function of inorganic content. Error bars represent one standard deviation of the acquired breakdown data. The breakdown strength for blend and HNP films follow distinct trends with increasing inorganic content fraction. The non-electronic grade PS exhibited a characteristic breakdown strength of 175 V/μm, and was used as the basis for comparing all PNC breakdown values. PS + BaTiO$_3$ traditional blend films displayed a marked reduction in breakdown strength, decreasing from 139 V/μm at 3% v/v down to

93 V/μm at 25% v/v loading – a nearly 50% reduction in E_{BD} as compared to neat PS. The breakdown strength for the HNP PS@BaTiO$_3$ and PS@BaTiO3 + PS films ranged from 143 V/μm to 164 V/μm, for loading fractions up to 22% v/v. The overall maintenance of breakdown strength across BaTiO$_3$ loading fractions for the HNP samples is notably different than observed for the analogous PS + BaTiO$_3$ blends. Furthermore, it should be emphasized that the 3 and 7% v/v HNP samples are, in fact, hybrid systems where free homopolymer chains were added to reduce volume fraction. Their breakdown behavior seems to lie in-between pure HNP and pure blend values, implying that uniformity in particle spacing and high molecular weight surface functionalization may play distinct roles in dielectric failure. PS@TiO$_2$ HNP samples were also studied with even higher inorganic content, up to 39% v/v. A decreasing trend was also observed for E_{BD}; films yielded a 167 V/μm breakdown strength at 13% v/v and 114 V/μm at 39% v/v. Interestingly, the TiO$_2$ and BaTiO$_3$ HNP films follow similar breakdown strength trends with increasing inorganic loading fractions. These results contrast with previous experiments performed on silica/electronic grade PS nanocomposite films, where the different PNC architectures showed similar breakdown values.[17]

Energy storage efficiencies measured for PS + BaTiO$_3$ blends and PS@BaTiO$_3$ HNPs are shown as a function of applied electric field for multiple inorganic volume fractions in Fig. 6. Efficiency was determined by integrating polarization loop areas; full polarization loop data for BaTiO$_3$/PS PNCs are shown in Supporting Information, Fig. S6. Discharge efficiency was comparable for 3% v/v PS@BaTiO$_3$ + PS and 4% v/v PS + BaTiO$_3$ and maintain a value of >85% for applied fields up to 125 V/μm. Differences between blends and matrix-free HNPs are evident at higher BaTiO$_3$ volume fractions. Significant drop-offs in efficiency are observed for the 15 and 25% v/v PS + BaTiO$_3$ blends when electric fields greater than 75 V/μm are applied, reaching a minimum of 81% at 84 V/μm. Conversely, PS@BaTiO$_3$ HNPs at 14 and 22% v/v loading deliver at least 88% efficiency above 100 V/μm. These results mirror low-ε PS/SiO$_2$ nanocomposites, where 15% v/v PS + SiO$_2$ blends exhibited degraded energy storage efficiencies when driven above 100 V/μm, while 18% v/v PS@SiO$_2$ HNPs maintained >90% efficiency, even at 200 V/μm.[22]

Overall, these findings imply that when introducing high-ε nanofillers and achieving comparable overall morphology, adopting a polymer grafting approach yields enhanced dielectric breakdown performance when compared to traditional blending. Furthermore, HNP films produced using the high ε nanoparticles (BaTiO$_3$ and TiO$_2$) followed the same trend in E_{BD} as a function of inorganic content. This contrasts previous conclusions from silica-based PNCs that any improvement in increasing minimum particle–particle separation afforded by HNP architectures did not ultimately impact breakdown strength.[22,30] The clear difference between these studies is the relative permittivity of the dispersed nanoparticles: silica ($\varepsilon_r = 4$) vs BaTiO$_3$ and TiO$_2$ ($\varepsilon_r = 150$ and 80, respectively). Therefore, we surmise that the relative permittivity between inclusion and host is the primary factor causing the diverging behavior in these two systems.
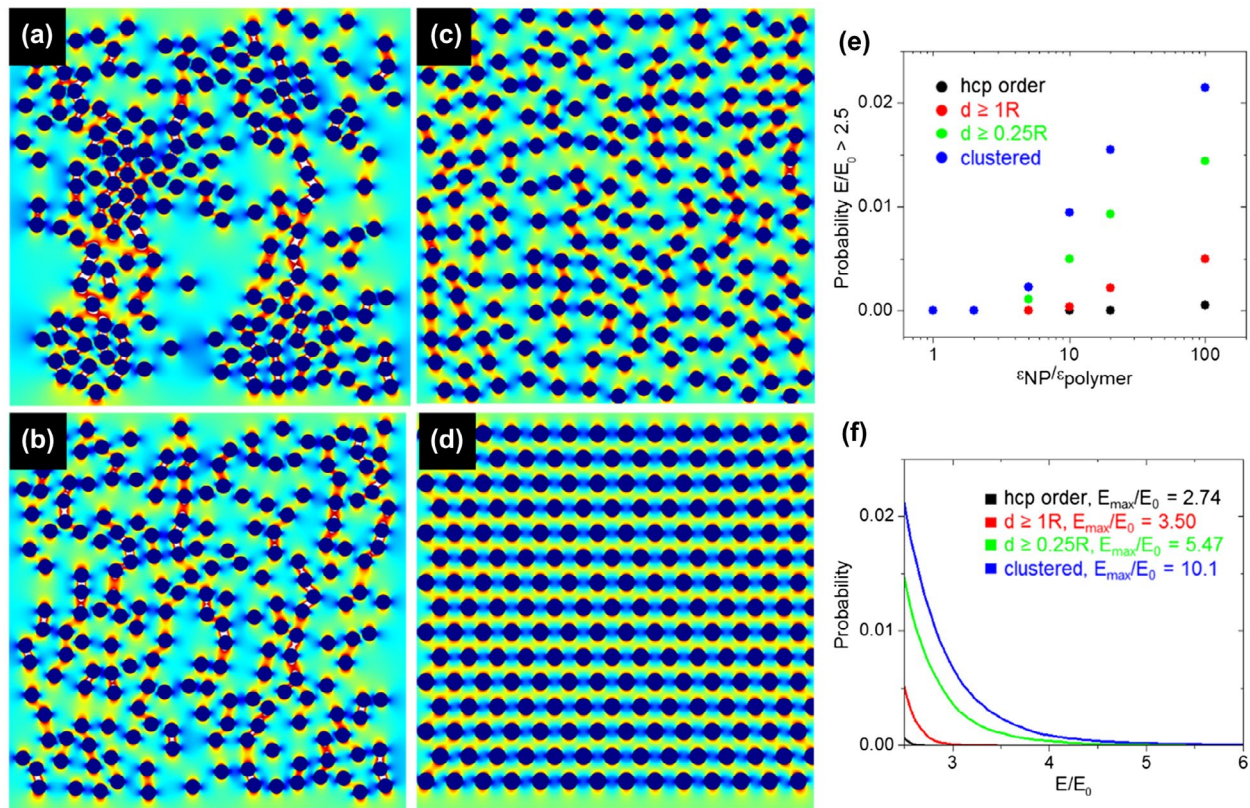
6

Figure 7 2D simulated electric field distributions for 200 particles with permittivity ratio of 100:1. *a* Clustered particles, where minimum particle separation, *d*, is greater than 0.001*R*, *b* dispersed particles where *d* > 0.25*R* (representing blended films), *c* where *d* > *R* (representing HNP films), and *d* an idealized hexagonally closed packed structure. Colors correspond to normalized field intensity E/E_0, where white regions are areas where $E/E_0 > 3$. *e* Probability of finding a region where $E/E_0 > 2.5$, as a function of permittivity ratio. *f* Cumulative probability for finding a region with field exclusion greater than E/E_0

COMSOL simulations were performed to illustrate the impact of nanoparticle permittivity on field exclusion behavior. Fig. 7 highlights 2D simulations where particles are arranged to approximate four different nanocomposite morphologies. In case 1, particles are allowed to aggregate and form clustered regions (modeling a poor blend); case 2, particles are separated by a distance of at least ¼ of a particle radius ($d \geq 0.25R$, representative of well blended films); case 3, where particles are separated by a full particle radius ($d \geq R$, modeling an HNP film); and case 4, which is an idealized hexagonal close-packed system. A high dielectric contrast of $\varepsilon_{NP}/\varepsilon_{poly} = 100$ reflects the contrast seen between $BaTiO_3$ and polystyrene. As particle location becomes more randomized and particle–particle distance diminishes, the probability of finding regions of high field intensity (defined here as $E/E_0 > 2.5$) rises dramatically as the dielectric contrast between particle and matrix increases. Conversely, no appreciable rise in probability is seen when contrast is increased if particles are not allowed to come into close contact. Similar trends are observed when searching for the maximum value of E/E_0. Samples allowed to form larger, denser particle clusters will yield higher E/E_0 values, which becomes greatly enhanced as $\varepsilon_{NP}/\varepsilon_{polymer}$ deviates from unity. Thus, in our current study, we can understand how high-ε PS/ $BaTiO_3$ nanocomposites benefit from the HNP architecture due to its ability in limiting close particle packing and mitigate field enhancement. The increased nanoparticle dispersion most likely prevents preferential charge migration along the surface of very large filler aggregates. Comparatively, lower ε silica/PS nanocomposites do not draw similar gains

in dielectric performance, since field enhancement remains weak regardless of particle–particle spacing.

Conclusions

We have demonstrated that grafting matrix polymers to nanoparticle surfaces has significant benefits in maintaining dielectric breakdown strength and improving dielectric loss for $BaTiO_3$ and TiO_2-based nanocomposite devices. At 22% inorganic loading, HNP PS@$BaTiO_3$ films exhibited breakdown strength 18% lower than unfilled polystyrene, whereas blended PS + $BaTiO_3$ films showed a nearly 50% reduction. Thus, despite the relative similarities in morphology as observed by X-ray scattering, HNP PS@$BaTiO_3$ films maintain breakdown strength better than blended composites for inorganic contents sufficient to provide enhanced composite permittivity. This equates to a theoretical energy storage density ($U = \frac{1}{2}\varepsilon_0\varepsilon_r E_{BD^2}$) that is 2 times unfilled polystyrene, and 4 times that of the blended $BaTiO_3$ polystyrene composite at a similar loading (22% v/v $BaTiO_3$). The simultaneous improvements to permittivity, while maintaining low dielectric loss at reasonable field strengths afforded by single component HNPs, are promising for improved capacitive energy densities for future energy storage applications.

The $BaTiO_3$ and TiO_2-based nanocomposites discussed here exhibit a large dielectric contrast between inorganic filler and polymer matrix host (>30), which is significantly larger than silica-based composite films (<2) that have been studied previously. The findings on silica/polystyrene composites indicate

that the route (HNP vs. blending) to a well-dispersed morphology has at most a minor impact on breakdown strength trends with nanoparticle volume fraction; however, polymer grafting does positively influence dielectric loss and efficiency properties. In contrast, observations with well-dispersed high permittivity fillers are most likely attributed to local nanoparticle–nanoparticle structure and field exclusion effects, which are exacerbated in systems where particles can come closer into contact. Single component HNP architectures, which have previously shown improvement over traditional blends in silica-based PNC systems due to reduced dielectric loss, have the added benefit of higher breakdown strength by forcing particles to remain further apart in $BaTiO_3$ and TiO_2 nanocomposites. These findings clearly point to the performance benefits of functionalizing the nanoparticle surface with high molecular weight polymer for polymer nanostructured dielectrics.

Supplementary material

The supplementary material for this article is available online at http://dx.doi.org/10.1080/20550324.2016.1223913.

Disclosure statement

No potential conflict of interest was reported by the authors.

References

1. J. K. Nelson, ed.: 'Dielectric polymer nanocomposites'; 2010, New York, NY, Springer.
2. Q. Wang and L. Zhu: 'Polymer nanocomposites for electrical energy storage', *J. Polym. Sci. B Polym. Phys.*, 2011, **49**, 1421–1429.
3. M. A. Firestone, S. C. Hayden and D. L. Huber: 'Greater than the sum: synergy and emergent properties in nanoparticle–polymer composites', *MRS Bull.*, 2015, **40**, 760–767.
4. J. S. Meth, S. G. Zane, C. Chi, J. D. Londono, B. A. Wood, P. Cotts, M. Keating, W. Guise and S. Weigand: 'Development of Filler Structure in Colloidal Silica-Polymer Nanocomposites', *Macromolecules*, 2011, **44**, 8301–8313.
5. J. P. Calame: 'Finite difference simulations of permittivity and electric field statistics in ceramic-polymer composites for capacitor applications', *J. Appl. Phys.*, 2006, **99**, 084101.
6. P. Kim, N. M. Doss, J. P. Tillotson, P. J. Hotchkiss, M.-J. Pan, S. R. Marder, J. Li, J. P. Calame and J. W. Perry: 'High energy density nanocomposites based on surface-modified BaTiO3 and a ferroelectric polymer', *ACS Nano*, 2009, **3**, 2581–2592.
7. H. Tang and H. A. Sodano: 'Ultra High Energy Density Nanocomposite Capacitors with Fast Discharge Using Ba0.2Sr0.8TiO3 Nanowires', *Nano Lett.*, 2013, **13**, 1373–1379.
8. G. Y. Wang, X. Y. Huang and P. K. Jiang: 'Tailoring dielectric properties and energy density of ferroelectric polymer nanocomposites by high-k nanowires', *ACS Appl. Mater. Interfaces*, 2015, **7**, 18017–18027.
9. S. P. Fillery, H. Koerner, L. Drummy, E. Dunkerley, M. F. Durstock, D. F. Schmidt and R. A. Vaia: 'Nanolaminates: Increasing dielectric breakdown strength of composites', *ACS Appl. Mater. Interfaces*, 2012, **4**, 1388–1396.

10. Z. M. Dang, J. K. Yuan, S. H. Yao and R. J. Liao: 'Flexible nanodielectric materials with high permittivity for power energy storage', *Adv. Mater.*, 2013, **25**, 6334–6365.
11. L. A. Fredin, Z. Li, M. A. Ratner, M. T. Lanagan and T. J. Marks: 'Enhanced energy storage and suppressed dielectric loss in oxide core-shell-polyolefin nanocomposites by moderating internal surface area and increasing shell thickness', *Adv. Mater.*, 2012, **24**, 5946–5953.
12. X. Y. Huang and P. K. Jiang: 'Core-shell structured high-k polymer nanocomposites for energy storage and dielectric applications', *Adv. Mater.*, 2015, **27**, 546–554.
13. K. Yang, X. Huang, M. Zhu, L. Xie, T. Tanaka and P. Jiang: 'Combining RAFT polymerization and thiol–ene click reaction for core–shell structured polymer@ BaTiO3 nanodielectrics with high dielectric constant, low dielectric loss, and high energy storage capability', *ACS Appl. Mater. Interfaces*, 2014, **6**, 1812–1822.
14. S. Virtanen, T. M. Krentz, J. K. Nelson, L. S. Schadler, M. Bell, B. Benicewicz, H. Hillborg and S. Zhao: 'Dielectric breakdown strength of epoxy bimodal-polymer-brush-grafted core functionalized silica nanocomposites', *IEEE Trans. Dielectr. Electr. Insul.*, 2014, **21**, 563–570.
15. N. J. Fernandes, H. Koerner, E. P. Giannelis and R. A. Vaia: 'Hairy nanoparticle assemblies as one-component functional polymer nanocomposites: opportunities and challenges', *MRS Commun.*, 2013, **3**, 13–29.
16. P. Tao, Y. Li, A. Rungta, A. Viswanath, J. N. Gao, B. C. Benicewicz, R. W. Siegel and L. S. Schadler: 'TiO2 nanocomposites with high refractive index and transparency', *J. Mater. Chem.*, 2011, **21**, 18623–18629.
17. C. M. Hui, J. Pietrasik, M. Schmitt, C. Mahoney, J. Choi, M. R. Bockstaller and K. Matyjaszewski: 'Surface-initiated polymerization as an enabling tool for multifunctional (nano-)engineered hybrid materials', *Chem. Mater.*, 2014, **26**, 745–762.
18. M. N. Tchoul, S. P. Fillery, H. Koerner, L. F. Drummy, F. T. Oyerokun, P. A. Mirau, M. F. Durstock and R. A. Vaia: 'Assemblies of titanium dioxide-polystyrene hybrid nanoparticles for dielectric applications', *Chem. Mater.*, 2010, **22**, 1749–1759.
19. S. Siddabattuni, T. P. Schuman and F. Dogan: 'Dielectric properties of polymer-particle nanocomposites influenced by electronic nature of filler surfaces', *ACS Appl. Mater. Interfaces*, 2013, **5**, 1917–1927.
20. S. A. Paniagua, Y. Kim, K. Henry, R. Kumar, J. W. Perry and S. R. Marder: 'Surface-initiated polymerization from barium titanate nanoparticles for hybrid dielectric capacitors', *ACS Appl. Mater. Interfaces*, 2014, **6**, 3477–3482.
21. C. A. Grabowski, S. P. Fillery, N. M. Westing, C. Z. Chi, J. S. Meth, M. F. Durstock and R. A. Vaia: 'Dielectric breakdown in silica-amorphous polymer nanocomposite films: the role of the polymer matrix', *ACS Appl. Mater. Interfaces*, 2013, **5**, 5486–5492.
22. C. A. Grabowski, H. Koerner, J. S. Meth, A. Dang, C. M. Hui, K. Matyjaszewski, M. R. Bockstaller, M. F. Durstock and R. A. Vaia: 'Performance of dielectric nanocomposites: matrix-free, hairy nanoparticle assemblies and amorphous polymer-nanoparticle blends', *ACS Appl. Mater. Interfaces*, 2014, **6**, 21500–21509.
23. R. L. Brutchey and D. E. Morse: 'Template-free, low-temperature synthesis of crystalline barium titanate nanoparticles under bio-inspired conditions', *Angew. Chem. Int. Ed. Engl.*, 2006, **45**, 6564–6566.
24. C. W. Beier, M. A. Cuevas and R. L. Brutchey: 'Effect of surface modification on the dielectric properties of BaTiO3 nanocrystals', *Langmuir*, 2009, **26**, 5067–5071.
25. ASTM D 149 standard test method for dielectric breakdown voltage and dielectric strength of solid electrical insulating materials at commercial power frequencies, in Annual book of ASTM standards1992, Conshohocken, PA, American Society for Testing and Materials.
26. S. J. Laihonen, U. Gafvert, T. Schutte and U. W. Gedde: 'DC breakdown strength of polypropylene films: area dependence and statistical behavior'. *IEEE Trans. Dielectr. Electr. Insul.*, 2007, **14**, 275–286.
27. J. K. Percus and G. J. Yevick: 'Analysis of classical statistical mechanics by means of collective coordinates', *Phys. Rev.*, 1958, **110**, 1–13.
28. D. A. G. Bruggeman: 'Berechnung Verschiedener Physikalischer Konstanten von Heterogenen Substanzen. I. Dielektriztatskonstanten und Leitfahigkeiten der Mischkorper aus Isotropen Substanzen [Calculation of various physics constants in heterogenous substances: I. Dielectricity constants and conductivity of mixed bodies from isotropic substances]'. *Ann. Phys. (N.Y.)*, 1935, **416**, 636–664.
29. L. Zhu: 'Exploring strategies for high dielectric constant and low loss polymer dielectrics', *J. Phys. Chem. Lett.*, 2014, **5**, 3677–3687.
30. C. A. Grabowski, H. Koerner and R. A. Vaia: 'Enhancing dielectric breakdown strength: structural relaxation of amorphous polymers and nanocomposites', *MRS Commun.*, 2015, **5**, 205–210.

8